**Supporting Information (SI)**

**Achieving high energy density for lithium-ion battery anodes by Si/C**

**nanostructures design**

Xingshuai Lv, Wei Wei[*], Baibiao Huang and Ying Dai[*]

School of Physics, State Key Laboratory of Crystal Materials, Shandong University,

250100 Jinan, China

[*] Corresponding authors

weiw@sdu.edu.cn (W. Wei)

daiy60@sdu.edu.cn (Y. Dai)

**Contents**

**Table S1** Comparison of lattice constants of $g$-SiC$_2$ and $g$-SiC$_3$ with previous theoretical results. "–" represents that there is no corresponding result for $g$-SiC$_2$ or $g$-SiC$_3$. The unit is Å.

|  | This work | Ref. 35 | Ref. 36 |
|---|---|---|---|
| $g$-SiC$_2$ | 5.02 | 5.019 | – |
| $g$-SiC$_3$ | 5.62 | – | 5.633 |

**Table S2** Adsorption energies on various possible adsorption sites. The most stable adsorption sites are highlighted in red. For C1 sites of $g$-SiC$_2$ and $g$-SiC$_3$, Li atoms will move to C2 and H1 sites after the optimization, respectively. The unit is eV.

|  | C1 | C2 | Si | H | H1 | H2 |
|---|---|---|---|---|---|---|
| $g$-SiC$_2$ | −1.71 (C2) | −1.71 | −1.25 | <span style="color:red">−2.14</span> | – | – |
| $g$-SiC$_3$ | −2.24 (H1) | – | −1.54 | – | <span style="color:red">−2.24</span> | −1.95 |

**Table S3** Adsorption energies at different Li coverages. The unit is eV.

|  | 1×1 | 2×1 | 2×2 | 3×2 | 3×3 |
|---|---|---|---|---|---|
| $g$-SiC$_2$ | −2.14 | −2.21 | −2.25 | −2.27 | −2.28 |
| $g$-SiC$_3$ | −2.24 | −2.28 | −2.33 | −2.35 | −2.35 |

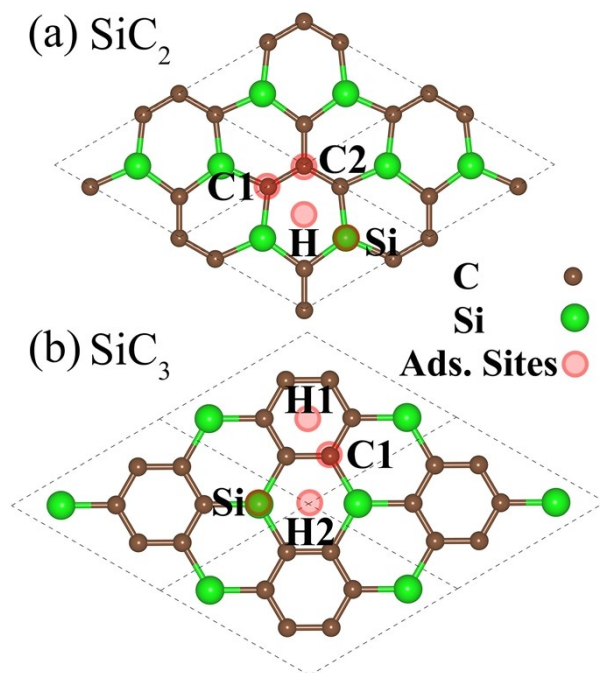**Figure S1** Schematic representations of the (2×2) supercells of (a) *g*-SiC$_2$ and (b) *g*-SiC$_3$. Small (Brown) and large (green) balls represent carbon and Si atoms, respectively.
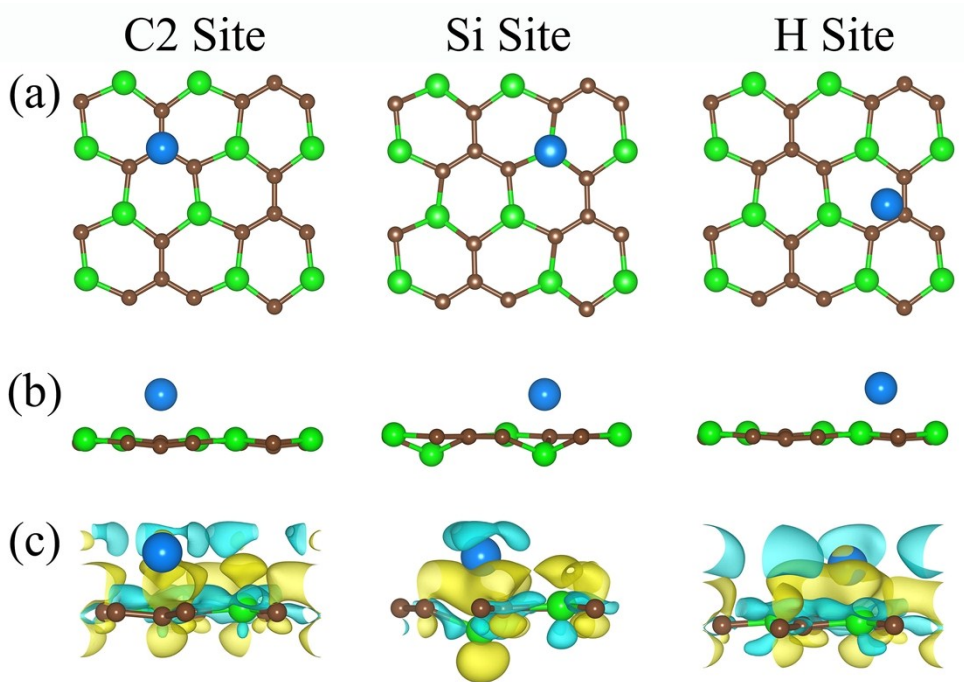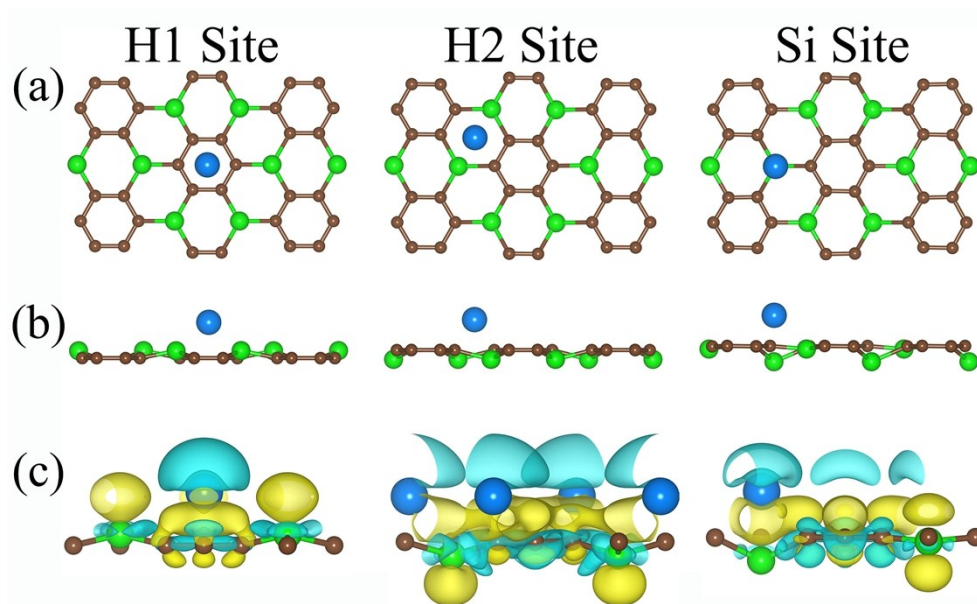
**Figure S2** (a) Top and (b) side views of three high-symmetry Li adsorption sites (C2, Si and H sites) on $g$-SiC$_2$. (c) Corresponding difference charge density. The yellow and blue areas represent electron gains and losses. The difference charge density ($\Delta\rho$) is calculated by $\Delta\rho = \rho_{total} - \rho_{SG} - \rho_{Li}$, where $\rho_{total}$, $\rho_{SG}$ and $\rho_{Li}$ are the total charge of the system, siligraphene and lithium atom, respectively.

**Figure S3** (a) Top and (b) side views of three high-symmetry Li adsorption sites (C2, Si and H sites) on $g$-SiC$_3$. (c) Corresponding difference charge density.



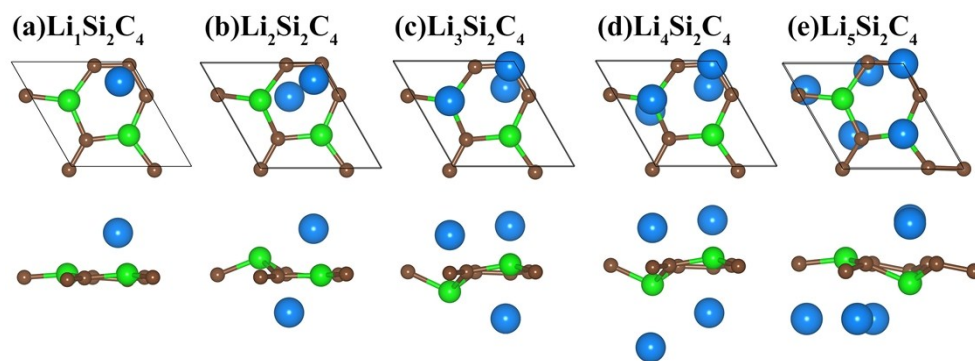**Figure S4** The most stable configurations of different $n$ ($n$ = 1, 2, 3, 4 and 5) of Li$_n$Si$_2$C$_4$.

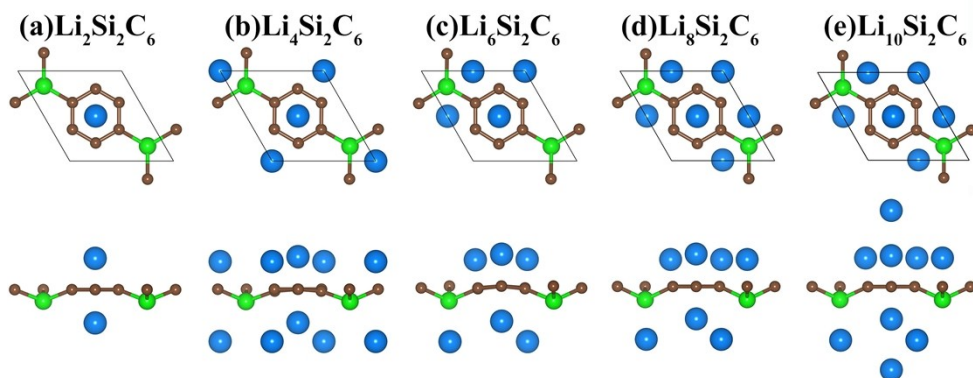**Figure S5** The most stable configurations of different $n$ ($n$ = 2, 4, 6, 8 and 10) of $Li_xSi_2C_6$.
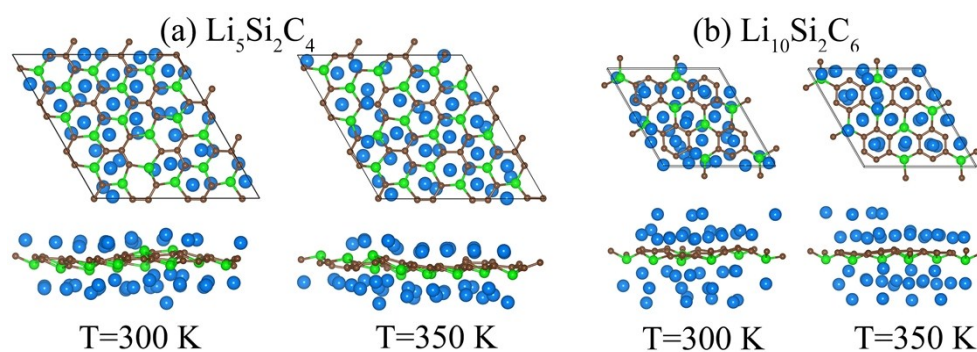


**Figure S6** Snapshots of the final configurations of (a) $Li_5Si_2C_4$ and (b) $Li_{10}Si_2C_6$ at temperatures of 300 and 350 K at the end of 10 ps AIMD simulations.
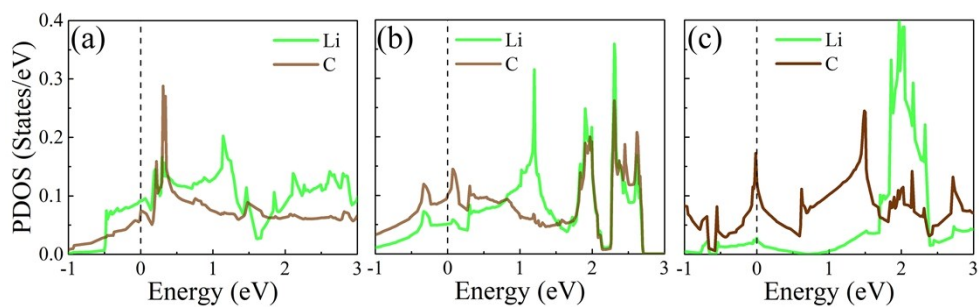
**Figure S7** Projected density of states (PDOS) of Li adsorption on (a) graphene, (b) $g$-SiC$_2$ and (c) $g$-SiC$_3$. The Fermi level is set to zero.
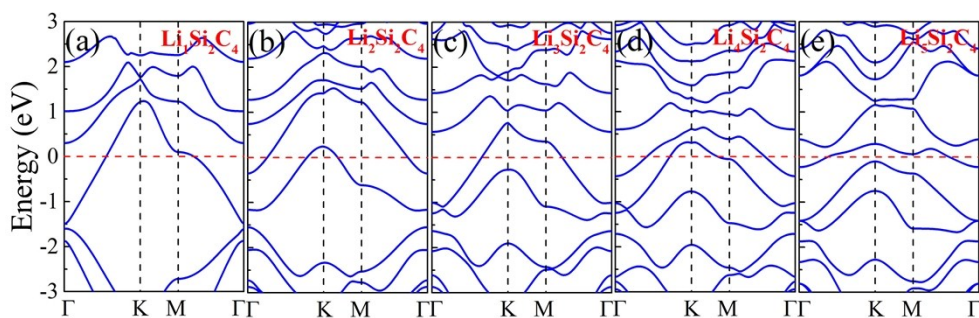


**Figure S8** Band structures of (a) Li$_1$Si$_2$C$_4$, (b) Li$_2$Si$_2$C$_4$, (c) Li$_3$Si$_2$C$_4$, (d) Li$_4$Si$_2$C$_4$ and (e) Li$_5$Si$_2$C$_4$, respectively. The Fermi level is set to zero.
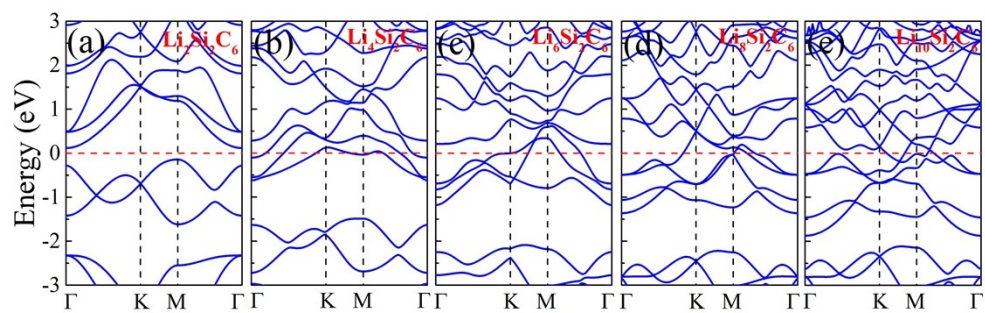
**Figure S9** Band structures of (a) $Li_2Si_2C_6$, (b) $Li_4Si_2C_6$, (c) $Li_6Si_2C_6$, (d) $Li_8Si_2C_6$ and

(e) $Li_{10}Si_2C_6$, respectively. The Fermi level is set to zero.